

# The Potential of a Radiosensitive Intracerebral Probe to Monitor $^{18}\text{F}$ -MPPF Binding in Mouse Hippocampus In Vivo

Aurélien Desbrée<sup>1,2</sup>, Mathieu Verdurand<sup>3</sup>, Jeremy Godart<sup>1</sup>, Albertine Dubois<sup>4</sup>, Roland Mastroianni<sup>1</sup>, Frédéric Pain<sup>1</sup>, Laurent Pinot<sup>1</sup>, Thierry Delzescaux<sup>4</sup>, Hiram Gurden<sup>1</sup>, Luc Zimmer<sup>3</sup>, and Philippe Lanièce<sup>1</sup>

<sup>1</sup>IMNC, UMR8165 CNRS-Université of Paris 7 and Paris 11, Orsay, France; <sup>2</sup>LEDI, IRSN, BP17, 92262 Fontenay aux Roses, France ;

<sup>3</sup>Laboratory of Neuropharmacology FRE CNRS 3006, University of Lyon, and CERMEP-Biomedical Cyclotron, Lyon, France; and

<sup>4</sup>MIRCE, URA CEA-CNRS 2210, Orsay, France

As mouse imaging has become more challenging in preclinical research, efforts have been made to develop dedicated PET systems. Although these systems are currently used for the study of physiopathologic murine models, they present some drawbacks for brain studies, including a low temporal resolution that limits the pharmacokinetic study of radiotracers. The aim of this study was to demonstrate the ability of a radiosensitive intracerebral probe to measure the binding of a radiotracer in the mouse brain in vivo. **Methods:** The potential of a probe 0.25 mm in diameter for pharmacokinetic studies was assessed. First, Monte Carlo simulations followed by experimental studies were used to evaluate the detection volume and sensitivity of the probe and its adequacy for the size of loci in the mouse brain. Second, ex vivo autoradiography of 5-hydroxytryptamine receptor 1A (5-HT<sub>1A</sub>) receptors in the mouse brain was performed with the PET radiotracer 2'-methoxyphenyl-(N-2'-pyridinyl)-p-<sup>18</sup>F-fluorobenzamidoethylpiperazine (<sup>18</sup>F-MPPF). Finally, the binding kinetics of <sup>18</sup>F-MPPF were measured in vivo in both the hippocampus and the cerebellum of mice. **Results:** Both the simulations and the experimental studies demonstrated the feasibility of using small probes to measure radioactive concentrations in specific regions of the mouse brain. Ex vivo autoradiography showed a heterogeneous distribution of <sup>18</sup>F-MPPF consistent with the known distribution of 5-HT<sub>1A</sub> in the mouse brain. Finally, the time-activity curves obtained in vivo were reproducible and validated the capacity of the new probe to accurately measure <sup>18</sup>F-MPPF kinetics in the mouse hippocampus. **Conclusion:** Our results demonstrate the ability of the tested radiosensitive intracerebral probe to monitor binding of PET radiotracers in anesthetized mice in vivo, with high temporal resolution suited for compartmental modeling.

**Key Words:**  $\beta$  microprobe; mouse; <sup>18</sup>F-MPPF; 5-HT<sub>1A</sub> receptors; small-animal imaging

**J Nucl Med 2008; 49:1155–1161**

DOI: 10.2967/jnumed.107.050047

The last 20 y have seen the emergence of many animal models that mimic human diseases (tumor growth, neurodegenerative disease, or neuropsychiatric disorders) and are used to investigate and propose new therapeutic approaches to these diseases (1). The murine models are of great interest because they are particularly suited to the application of molecular biology strategies such as knock-out and knock-in, generating many types of transgenic strains (2,3). In following disease progression and staging therapeutic protocols in vivo, the development of specific imaging techniques is essential for proper in vivo detection and quantification of molecular changes during gene expression (4). Radioactive techniques and, more particularly, PET are efficient ways to address this problem because they can provide quantitative information about in vivo biologic processes at the molecular level. In this context, many groups have focused on adapting PET tomographs—initially developed for human imaging, and more recently for rat studies—to overcome the specific constraints of the mouse. Although some interesting and promising results have already been obtained with dedicated small-animal PET (5–7), the available scanners suffer from drawbacks such as their limited sensitivity, which impairs their temporal resolution, especially at the end of the experiment, when radioactive signals become low.

In this study, we proposed an alternative to PET for mouse brain studies—the use of a local probe sensitive to  $\beta$ -radioactivity ( $\beta$  microprobe; Biospace Lab SA). This low-cost technology, which was initially developed for PET measurements of the rat brain, has successfully been used in pharmacokinetic and pharmacodynamic studies (8–12) and for quantitative measurements of glucose metabolism or cerebral blood flow (13–15) in rats. Here, we report the development of this technology for use in mice. First, we performed theoretic experiments conceiving and characterizing a 0.25-mm-diameter prototype suited for the mouse brain. Second, we characterized 2'-methoxyphenyl-(N-2'-pyridinyl)-p-<sup>18</sup>F-fluorobenzamidoethylpiperazine (<sup>18</sup>F-MPPF) binding in the

Received Jan. 9, 2008; revision accepted Mar. 4, 2008.

For correspondence or reprints contact: Philippe Lanièce, Laboratoire Imagerie et Modélisation en Neurobiologie et Cancérologie, CNRS UMR8165, Université Paris-Sud, 91406 Orsay Cedex, France.

E-mail: [laniece@imnc.in2p3.fr](mailto:laniece@imnc.in2p3.fr)

COPYRIGHT © 2008 by the Society of Nuclear Medicine, Inc.

mouse brain with *ex vivo* autoradiography and performed an *in vivo* pharmacokinetics study in anesthetized mice.  $^{18}\text{F}$ -MPPF is a well-known 5-hydroxytryptamine receptor 1A ( $5\text{-HT}_{1\text{A}}$ ) PET radiotracer used in preclinical studies on rats (10,11,12,16,17).  $^{18}\text{F}$ -MPPF is particularly suited to the development of the  $\beta$  microprobe for mouse applications because we have already reported time–activity curves for this radioligand in the rat brain using  $\beta$  microprobe technology (10–12). In addition, this radiotracer is considered to be of great interest for mouse models presenting  $5\text{-HT}_{1\text{A}}$  deregulations such as depression (18,19).

## MATERIALS AND METHODS

### Monte Carlo Simulation

Simulations were performed using Geant4, developed at CERN. Initially developed for particle physics analysis, Geant4 has also proved beneficial in biomedical research (20,21). In this study, we investigated a sensitive fiber, 0.25 mm in diameter and 1 mm long, fused to a nonsensitive fiber of the same diameter. Both were simulated with polystyrene. To determine the sensitivity of the probe, we simulated  $^{18}\text{F}$  in brain tissues using a homogeneous cylindrical source. The detection volume of the probe (volume in which the positrons are detectable; see (22) for calculation details) was computed from the Geant4 simulation using MATLAB, version 6.5 (The MathWorks, Inc.). This provided the origin coordinates of the emitted particles and determined whether the emitted particle was detected by the probe. From the Monte Carlo results, we determined a 3-dimensional (3D) matrix with 75- $\mu\text{m}$  side voxels, representing the volume where the particles can be emitted. Each voxel corresponds to the ratio between particles detected by the probe and emitted particles, that is, the local detection volume  $\epsilon$ . The sensitivity was defined as the integral of the efficiency on the volume.

### Spectroscopy Setup

Preliminary experiments were performed to evaluate the optical signal delivered by the 0.25-mm-diameter probe. The mean number of photoelectrons generated by  $\beta$ -particles crossing the scintillating part of a fused fiber was measured from 5 fused-fiber samples. These values were compared with the mean number of photoelectrons measured from 5 reference samples based on scintillating fibers without interfaces. Double-clad optical fibers were manufactured by Bicon. Each fused fiber sample consists of a 2-mm-long BCF-12 scintillating fiber (peak emission wavelength at 435 nm) thermally fused to a 5-cm-long BCF-98 clear fiber. The end of the clear fiber was optically coupled to a photomultiplier tube (BURLE 8850; Burle Industries Inc.). A trigger signal was supplied by a second photomultiplier tube (R740; Hamamatsu) set in front of the end of the scintillating fiber and connected to a Nuclear Instrumentation Module discriminator. Fiber samples were irradiated with a  $^{204}\text{Tl}$  source ( $\beta$ -emitter, energy at maximum = 765 keV, mean energy = 244 keV) placed 5 mm from the scintillating fiber.

### Determination of Experimental Probe Sensitivity

Ten probes were calibrated in 16-mL aqueous  $^{18}\text{F}$  solution (2.3 MBq/mL) to determine the sensitivity of the 0.25-mm-diameter 1-mm-long probes. Corresponding values were expressed in kBq/mL.

### Animal Procedure

We used 4 male Swiss mice (body weight,  $30 \pm 3$  g). They were housed at standard temperature and humidity, in artificial light (light from 8 AM to 8 PM). All experiments were conducted according to European Community Council (EEC) guidelines and directives (86/09/EEC).

### Synthesis of $^{18}\text{F}$ -MPPF

$^{18}\text{F}$ -MPPF was synthesized with a radiochemical yield of 25% (decay-corrected) in an automated system (23), using the chemical pathway previously described (24). Chemical and radiochemical purity were determined by high-performance liquid chromatography (>98%). Specific activity from the injected radiotracer ranged from  $79 \times 10^3$  to  $332 \times 10^3$  MBq/ $\mu\text{mol}$ .

### $\beta$ microprobe System

The  $\beta$  microprobe is a local  $\beta$ -radioactivity counter that takes advantage of the limited range of  $\beta$ -particles within biologic tissues to define a detection volume in which the radioactivity is counted. A detailed description and discussion of the system can be found elsewhere (25,26). In this study, the probes were composed of a scintillating plastic fiber, with a 0.25-mm diameter and 1.0-mm length, fused to a clear fiber of the same diameter and mounted on a Delrin support (Luxeri). An optical guide 60 cm in length was used to connect the nonscintillating end of the probe to a photomultiplier tube (R7400P; Hamamatsu).

### Kinetics of $^{18}\text{F}$ -MPPF Binding

The mice were anesthetized (urethane, 1.8 g/kg intraperitoneally) and placed on a stereotactic frame; their temperature was controlled with a heating blanket ( $37^\circ\text{C} \pm 1^\circ\text{C}$ ). The stereotactic coordinates used to implant the probes in the hippocampus and in the cerebellum were based on the atlas of Paxinos and Franklin (27). The bregma point and the dura were the referenced points for anteroposterior, mediolateral, and dorsoventral coordinates. The coordinates for implantation of the probes were as follows: anteroposterior,  $-3.0$ ; mediolateral,  $+3.0$ ; and dorsoventral,  $-3.8$ , for the hippocampus and anteroposterior,  $-5.8$ ; mediolateral,  $-1.0$ ; and dorsoventral,  $-3.0$ , for the cerebellum. The cerebellum probe was implanted at an angle of  $20^\circ$  to allow placement of the 2 probes. Because of the sensitivity of the probe to external light, *in vivo* experiments were performed in darkness by covering the mouse's head with black sheets. For each acquisition,  $17.5 \pm 2.1$  MBq of  $^{18}\text{F}$ -MPPF (in a volume of about 0.2 mL of saline) were injected into the tail vein over a 30-s period. The catheter was washed immediately with a bolus of saline. Radioactivity concentrations in the brain were measured during 70 min. Time–activity curve data were then decay-corrected to the time of radiotracer injection and normalized to the percentage injected dose per gram.

The binding potential (BP) value was calculated using the classic Logan graphical method for ligands with reversible binding kinetics using the cerebellum as a receptor-free reference region (28). The BP value is derived from the slope of the linear regression of the Logan plot for  $t > 20$  min:

$$\begin{aligned} \frac{\int_0^t \text{Hippo}(t) dt}{\text{Hippo}(t)} &= \left(1 + \frac{k_3}{k_4}\right) \cdot \frac{\int_0^t \text{Cereb}(t) dt}{\text{Hippo}(t)} - \frac{1}{k_4} \\ &= (1 + \text{BP}) \frac{\int_0^t \text{Cereb}(t) dt}{\text{Hippo}(t)} - \frac{1}{k_4}, \end{aligned}$$

where Hippo(t) is the measured signal from the hippocampus (free ligand and ligand bound to  $5\text{-HT}_{1\text{A}}$  receptors), Cereb(t) is the

measured signal from the cerebellum (reference region with free ligand and no specific binding),  $k_3$  is the rate transfer constant from the free to bound compartment ( $\text{min}^{-1}$ ), and  $k_4$  is the rate transfer constant from the bound to the free compartments.

### Probe Placement Controls

After the acquisition, the anesthetized mice were killed by decapitation and the brain frozen in 2-methylbutane cooled to  $-40^\circ\text{C}$ . Cryostat sections (20  $\mu\text{m}$  thick) were cut across the hippocampus and the cerebellum and were thaw-mounted on slides. The sections were stained with cresyl blue, and the placement of the probes was matched on a stereotactic atlas of the mouse brain.

### 3D Reconstruction of Binding of $^{18}\text{F}$ -MPPF onto 5-HT<sub>1A</sub> Receptors in Mouse Brain

Twenty minutes after the intravenous injection of  $^{18}\text{F}$ -MPPF with an activity of 18 MBq, the mouse was sacrificed and its brain rapidly removed and frozen for autoradiography processing. Brain sections (20  $\mu\text{m}$  thick) encompassing the hippocampus and the dorsal raphe regions were cut using a cryomicrotome at  $-20^\circ\text{C}$ , mounted on Superfrost slides (Erie Scientific Co.), quickly dried, and exposed onto autoradiographic film (BioMax MR; Kodak) for 24 h. Sections were then stained with cresyl violet. Histologic and autoradiographic images were scanned at 1,200 dpi (ImageScanner and ImageMaster LabScan, version 3.00; Amersham Biosciences Europe). Anatomic and autoradiographic sections were automatically extracted from global scans and rigidly aligned using the block-matching method (29,30) as follows. First, each anatomic section was registered with the next section, leading by propagation to a coherent 3D anatomic volume. Second, each autoradiographic section was directly coregistered with its corresponding registered histologic section from the histologic volume to generate a consistent 3D radiopharmaceutical binding volume.

## RESULTS

### Feasibility, Development, and Characterization of 0.25-mm-Diameter Probes

As previously reported for rat prototypes of the  $\beta$  microprobe (25), the feasibility of using radiosensitive probes for mouse studies was primarily investigated. Because of the small size of the mouse brain ( $\sim 0.45$  g, vs.  $\sim 2$  g for the rat brain), we chose to develop a probe with 0.25-mm-diameter plastic fibers. These were chosen because plastic is compatible with brain implantations; the diameter is suited for the brain size, allows for fusion of plastic fibers, and is large enough to deliver an optical signal created by  $\beta$ -particles crossing the scintillating fiber; and scintillating and non-scintillating plastic fibers 0.25 mm in diameter are commercially available (Bicron). A 0.25-mm-diameter  $\beta$ -probe prototype was previously developed by Weber et al. (15) but was referenced only to rat applications and the use of  $^{15}\text{O}$ -H<sub>2</sub>O. Thus, feasibility was realized in 2 stages: in the first, the physical performances were theoretically determined; in the second, the possibility of fusing 0.25-mm-diameter fibers was tested.

Probe performance was assessed as follows. Detection volume and sensitivity (see "Materials and Methods") were established by simulating probes with a scintillating part 0.25 mm in diameter and 1 mm in length dipped into an  $^{18}\text{F}$  cylindrical positron source. The detection volume was 13  $\mu\text{L}$ . This was compared with the size of various cerebral loci in mice. As an example, Figure 1 illustrates the detection volume of a 0.25-mm-diameter probe for  $^{18}\text{F}$  and the superimposition of this detection volume with mouse brain frontal sections as if the 0.25-mm-diameter probe were implanted for an  $^{18}\text{F}$ -tracer measurement in the hippocampus and cerebellum. In this typical configuration, the use of the 0.25-mm-diameter probe is well suited for mouse recordings because the probe detection volume fits well with both locus sizes. The detection volume appeared to be consistent with mouse cerebral structures in general, which have volumes of less than 40  $\mu\text{L}$ .

The theoretic sensitivity of the mouse  $\beta$  microprobe was 0.109 cps/(kBq/mL). Because of the expected weakness of the optical signal obtained from  $\beta$ -particles crossing the scintillating 0.25-mm-diameter fiber, we used experimental measurements to estimate the actual sensitivity, taking into account potential signal losses expected in the complete setup (interfaces, photomultiplier efficiency, electronic threshold, and other factors). This result was imposed to establish fusion between the 0.25-mm-diameter plastic fibers. To make these new probes, we introduced and adapted a dedicated machine, previously used only to fuse fibers 0.5 and 1 mm in diameter (26). This adaptation allowed us to achieve fused samples at the price of low output (10% vs. 100% when using 0.5-mm-diameter fibers) but with an interface mechanically and optically optimized. To test this quality, we developed a specific low-light analyzer setup (see "Materials and Methods") that allowed us to quantify the signal. The maximum,  $7.8 \pm 0.9$  photoelectrons, and the mean,  $2.6 \pm 0.2$  photoelectrons, represented a 10% decrease in the mean number of photoelectrons, compared with the light intensity spectrum for reference samples (with no fusion). Thus, the fused interface caused a slight loss of light, consistent with observations for fibers of higher diameter, and the choice of thermal fusion to join the plastic scintillating fibers and the optical fibers was validated. In addition, with a mean number of photoelectrons consistently higher than 1, the expected signal should be sufficient for the recording of measurements with such a probe connected to the complete setup. We tested the probe in experimental conditions using the optical guide and the high-sensitivity and low-thermal-noise photomultiplier tube initially used for rat studies (26).

To this end, 10 probes were calibrated in 16 mL of  $^{18}\text{F}$  aqueous solution (2.3 MBq/mL). We obtained an experimental sensitivity of  $0.032 \pm 0.007$  cps/kBq/mL. This experimental sensitivity is more than 3 times lower than the theoretic value and, thus, more than 6 times lower than the sensitivity of the probes used for rat studies. This loss in sensitivity is a direct and expected result of the use of the

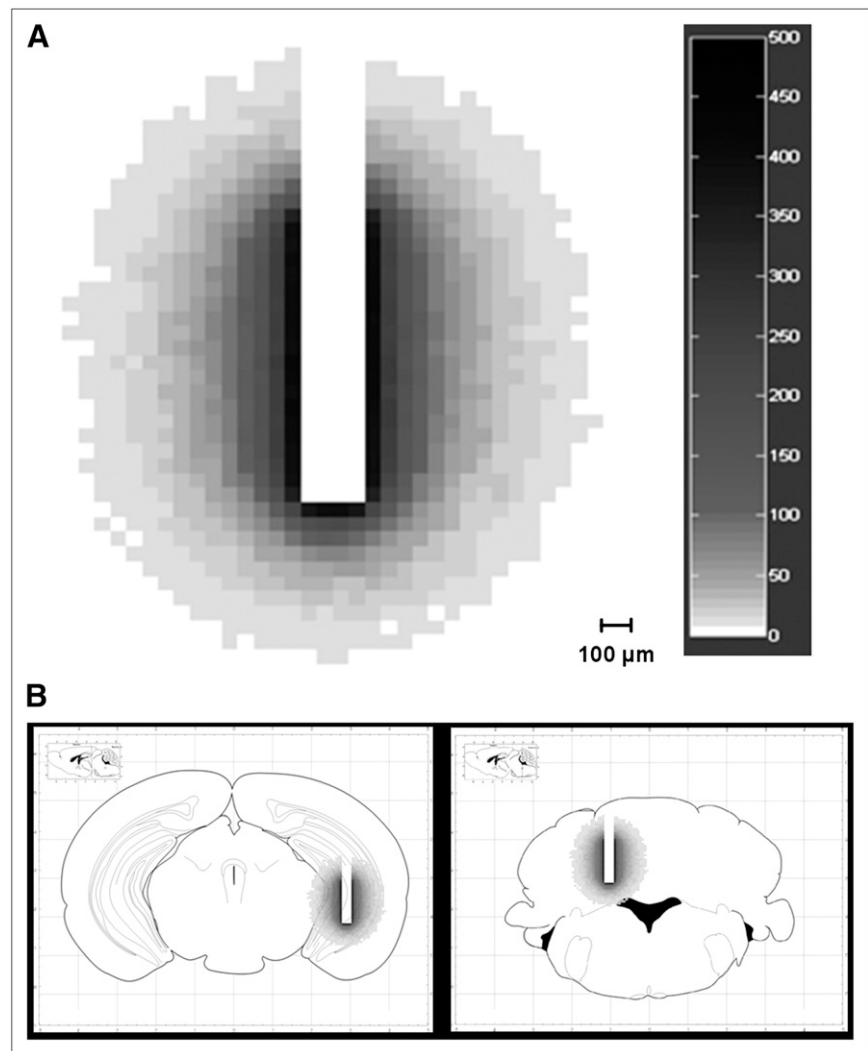


**FIGURE 1.** (A) Detection volume for 0.25-mm-diameter probe with 1.0-mm scintillating part dipped in  $^{18}\text{F}$  source. Scale is normalized to 1,000 events shot in a voxel. Horizontal bar scale represents 100  $\mu\text{m}$ . (B) Simulation of 0.25-mm-diameter probe and its corresponding detection volume superimposed onto brain mouse frontal sections adapted from Paxinos and Frankin (27) and showing ventral hippocampus (left panel) and cerebellum (right panel).

optical guide, the associated connections, and the electronics threshold, which substantially reduce the signal. Whereas almost all the signal is retained using a 500- $\mu\text{m}$ -diameter probe (with a mean number of 5 photoelectrons initially obtained using  $^{18}\text{F}$ ), 60% of the signal is lost using a 250- $\mu\text{m}$ -diameter probe, the sensitivity being at the limit of the recoverable signal.

#### Pharmacologic Validation of 0.25-mm-Diameter Probe

Before performing *in vivo* experiments, we determined the distribution of  $^{18}\text{F}$ -MPPF binding in the mouse brain by *ex vivo* autoradiography. This radioligand showed substantial accumulation in 5-HT<sub>1A</sub> regions such as the entorhinal cortex, the hippocampus, and the raphe (Fig. 2). In contrast, accumulation of  $^{18}\text{F}$ -MPPF in the cerebellum was negligible, confirming the low levels of receptor in this region. As well as confirming  $^{18}\text{F}$ -MPPF distribution, these findings helped to determine the optimal implantation site by allowing us to correlate the probe detection volume with the region of highest specificity in the hippocampus (Fig. 3).

*In vivo* experiments were performed on the basis of this *ex vivo* validation. Figure 4 shows mean ( $\pm$ SEM)  $^{18}\text{F}$ -MPPF radioactivity kinetic curves for the hippocampus and cerebellum of mice ( $n = 4$ ) and the corresponding specific binding curve deduced from subtraction of both the hippocampus and the cerebellum curves. The levels of radioactivity in the hippocampus increased over 10 min, reached a maximum, then decreased slowly with time, whereas radioactivity levels in the cerebellum peaked within 3 min after radioligand injection and then cleared rapidly. The amounts of  $^{18}\text{F}$ -MPPF, expressed as percentage injected dose per gram, reaching both the hippocampus and the cerebellum in mice are similar to those observed from autoradiographic data on rats (16):  $0.078 \pm 0.011$  and  $0.152 \pm 0.061$  for the hippocampus and  $0.025 \pm 0.005$  and  $0.036 \pm 0.013$  for the cerebellum, in mice and rats, respectively, at 30 min. The hippocampus-to-cerebellum ratios obtained with the mouse  $\beta$  microprobe were 3.06 at 15 min, 3.21 at 30 min, and 2.58 at 45 min after injection. These values are consistent with those previously obtained with the rat  $\beta$  microprobe (3.05,

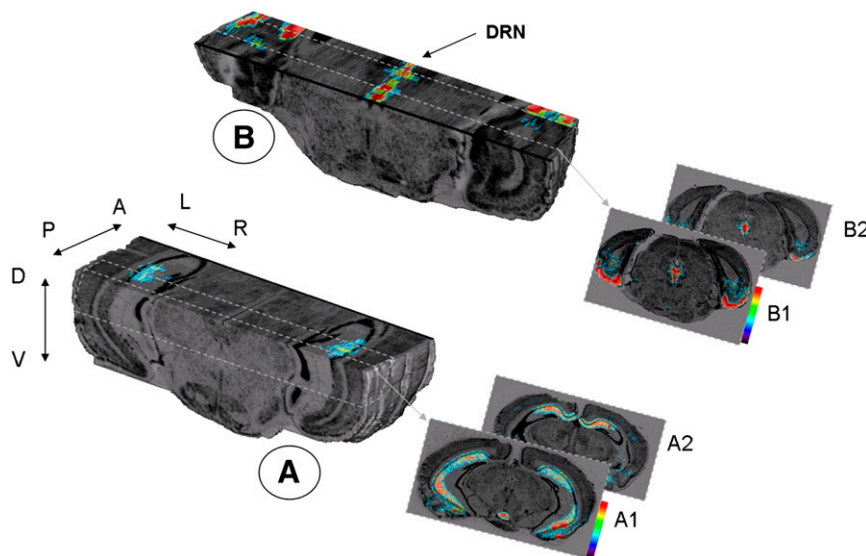


**FIGURE 2.** 3D postmortem imaging of radioligand distribution in mouse brain after injection of  $^{18}\text{F}$ -MPPF. (A) 3D reconstruction of  $^{18}\text{F}$ -MPPF binding in hippocampal region. Background black and white anatomic volumetric reconstruction of cresyl violet-stained sections shows bilateral location of 5-HT<sub>1A</sub> binding in mouse hippocampus. (A1 and A2) Representative coronal sections showing labeling in posterior/ventral (A1) and anterior/dorsal (A2) hippocampus. (B) 3D reconstruction of  $^{18}\text{F}$ -MPPF binding centered on dorsal raphe nucleus (DRN) also showing entorhinal cortex. (B1 and B2) Representative coronal sections showing labeling in posterior (B1) and anterior (B2) DRN. Pseudocolored digitized autoradiographs illustrate level of  $^{18}\text{F}$ -MPPF binding and are color-coded from low (blue) to high (red) binding. Arrow labels: A = anterior; P = posterior, L = left; R = right; D = dorsal; V = ventral.

3.65, and 3.58, respectively (24)) and autoradiography (3.05, 4.2, and 3, respectively (16)). For a quantitative comparison, we determined the BP of  $^{18}\text{F}$ -MPPF in the hippocampus of the mouse following the method previously proposed by Logan et al. (28) (see “Materials and Methods”): the mouse BP that we calculated was  $1.75 \pm 0.4$ . This mouse BP remains close to the rat BP value:  $2.3 \pm 0.6$  (11).

## DISCUSSION

Since the mid 1980s, the use of mouse models has become increasingly popular for the study of disease. In 2000, more than 90% of all mammals used for research worldwide were mice (31). Recently, many conventional and transgenic models have been developed to study disorders of the human central nervous system. For example, the possibility that serotonergic 5-HT<sub>1A</sub> deficiency plays a role in mood and anxiety disorders prompted studies to genetically manipulate 5-HT<sub>1A</sub> in mice (18,32). In this context, PET has become integral to the study of the integrative mammalian biology of disease (33). Nevertheless, although PET has already and successfully been used in mice for whole-body acquisitions, its current brain applications, requiring high spatial resolution and sensitivity, have met with some limitations. These led us to propose a mouse version of the  $\beta$  microprobe, which was initially designed for rat applications. This probe has specific properties allowing its use as a complement to small-animal PET in neurobiologic experiments on mice.

The aim of the present study was thus to demonstrate the potential benefits and capacity of the  $\beta$  microprobe for in vivo mouse experiments. To this end, we performed our study in 2 stages.

First, we designed and constructed a probe suitable for the mouse brain but limited in invasiveness. Although a 250- $\mu\text{m}$ -diameter plastic probe proved suitable for mouse cerebral PET studies, we also found that a probe of this

diameter had potential physical limitations. The rigidity of the probe approached the minimal threshold required for implantation in brain tissue, and the light signal delivered by the positron crossing the scintillating fiber was barely detectable with the photomultiplier tube. An elegant alternative was the use of inorganic scintillators such as lutetium oxyorthosilicate (LSO) with a larger stopping power for  $\beta$ -particles, allowing the probe diameter to be reduced. Using LSO, Woody et al. developed a 500- $\mu\text{m}$ -diameter probe for use specifically in rats (34). However, compared with plastic probes, LSO is more sensitive not only to positrons but also to 511-keV  $\gamma$ -rays. The energy threshold required to eliminate this significant background noise highly reduces the sensitivity of LSO probes especially for  $^{18}\text{F}$  tracers, with a maximum positron energy of 635 keV. Further studies should be performed to evaluate the potential of LSO probes 0.25 mm or less in diameter in mouse applications and, in particular, the influence on probe

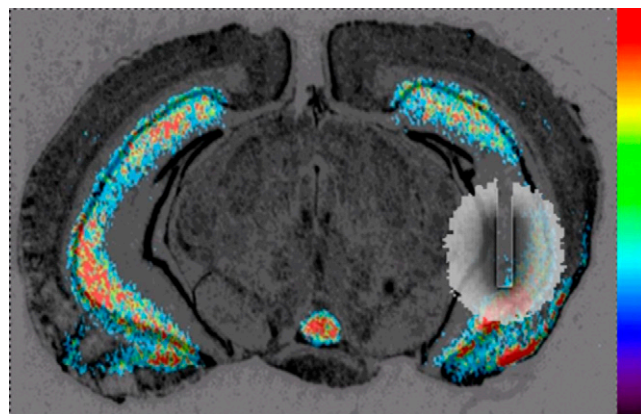
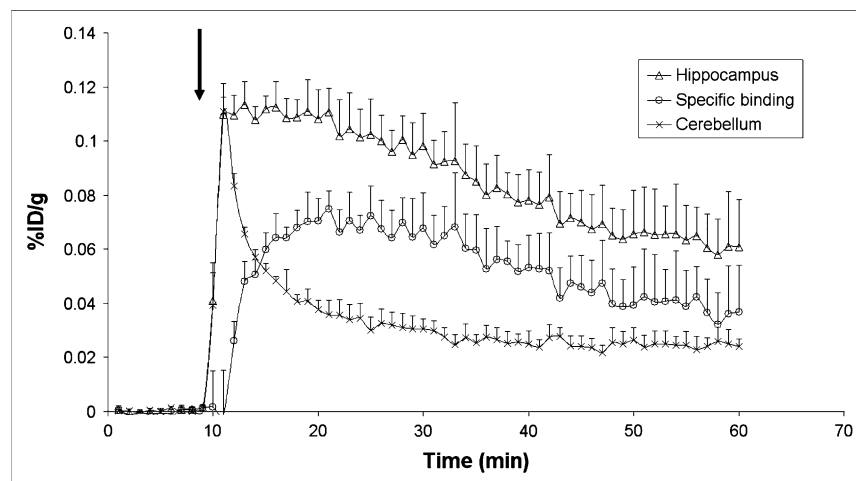


**FIGURE 3.** Simulation of 0.25-mm-diameter probe and its corresponding detection volume for implantation in mouse hippocampus.

**FIGURE 4.** Radioactivity kinetic curves measured by  $\beta$  microprobe in hippocampus and cerebellum of anesthetized mice after  $^{18}\text{F}$ -MPPF injection and corresponding specific binding curve deduced from subtraction of both hippocampus and cerebellum curves. Each point represents mean ( $\pm$ SEM) of radioactivity, expressed as percentage injected dose per gram for 4 mice. Arrow indicates time of radioligand injection. Data are averaged every minute for clarity.



sensitivity of  $\beta$ - and 511-keV  $\gamma$ -signal discrimination by energy threshold.

In the second stage of this study, we tested the capacity of our newly developed  $\beta$  microprobe prototypes to monitor the pharmacokinetics of a specific radiotracer in the brains of living mice. We used  $^{18}\text{F}$ -MPPF, a radiotracer that we previously used with the  $\beta$  microprobe in rat experiments and that has been widely validated for PET studies of 5-HT<sub>1A</sub> (17). Although it has previously been shown that regional distribution of this radioligand corresponds to the 5-HT<sub>1A</sub> distribution pattern of several species, including rats (9,10,12,16,35), cats (36), and humans (37), this study provides the first 3D reconstructions of the autoradiographic volumetric distribution of 5-HT<sub>1A</sub> in the mouse brain. These results are consistent with previous studies showing a similar 5-HT<sub>1A</sub> distribution pattern between different mammalian species and thus demonstrating the phylogenetic stability of the serotonergic neurotransmitter systems (38). In vivo experiments were performed, and  $^{18}\text{F}$ -MPPF specific binding was thus estimated as the difference between the concentration of radioligand in the region of interest (hippocampus, specific plus nonspecific) and the reference region (cerebellum, nonspecific). The time–radioactivity curves obtained with the  $\beta$  microprobe after intravenous  $^{18}\text{F}$ -MPPF administration were reproducible between mice (coefficient of variation, approximately 15%), showing a clear distinction between the hippocampus and the cerebellum. The hippocampus-to-cerebellum ratio increased linearly with time, approaching a value of 3 at 15 min, consistent with previous PET studies on rats (10,11). This ratio is compatible for future radiopharmacologic studies on mice, such as studies of radiotracer displacement, competition studies, or comparisons of the BP values between groups.

Thus, several applications may be considered for this methodology. The  $\beta$  microprobe is a versatile tool, used in rats for pharmacokinetic, pharmacodynamic, and physiologic studies (13); for determining arterial input function

for PET tracers (39); and for studies using other in vivo techniques, such as microdialysis or MRI, in combination (24). As previously discussed, quantitative analysis performed with PET cameras required an optimum balance between sensitivity and spatial resolution; the small size of mouse brain loci makes this balance difficult to achieve. Consequently, only a few studies have reported the use of PET cameras in mouse brain studies. Therefore, the  $\beta$  microprobe provides an attractive alternative to animal PET scanners. Although the  $\beta$  microprobe only defines a detection volume surrounding the radiosensitive probe rather than delivering images, our findings demonstrate that  $^{18}\text{F}$ -MPPF kinetic studies can be performed on live mice. Similarly to studies on rats, the  $\beta$  microprobe has several advantages in mouse studies: it is dynamic, acquiring kinetic data with high temporal resolution (every second) and thus allowing physiologic and pharmacologic processes to be measured; it is sensitive, detecting picomolar concentrations of radioligand in the brain; and although more often producing semiquantitative data, it is potentially quantitative.

## CONCLUSION

This is the first study to establish the  $\beta$  microprobe as a tool sufficiently sensitive to measure the specific binding of  $^{18}\text{F}$ -MPPF in the hippocampus of anesthetized mice. Our experimental results, together with our initial simulation studies, demonstrate that the probe is sensitive and selective and thus can be used for radiopharmacologic studies of PET radiotracer binding in the mouse brain. In particular, this new functional imaging approach will be invaluable for studies of serotonergic function in conventional or knock-out models of depression. Moreover, this methodology can be used to address a wide range of issues relevant to the PET exploration of neurotransmitter systems in mouse models of neurologic or psychiatric diseases.

## ACKNOWLEDGMENTS

We are grateful to Luc Magnier from Animage for his expert technical assistance. We thank Rhône-Alpes Genopole and Fondation Rhône-Alpes Futur, funded by the Réseau National des Genopoles. This work was supported by the academic funding program "Imagerie du Petit Animal" (Centre National de la Recherche Scientifique, Commissariat à l'Énergie Atomique).

## REFERENCES

- Koo V, Hamilton PW, Williamson K. Non-invasive in vivo imaging in small animal research. *Cell Oncol*. 2006;28:127–139.
- Paigen K. A miracle enough: the power of mice. *Nat Med*. 1995;1:215–220.
- Gao X, Kemper A, Popko B. Advanced transgenic and gene targeting approaches. *Neurochem Res*. 1999;24:1181–1188.
- Cherry SR. In vivo molecular and genomic imaging: new challenges for imaging physics. *Phys Med Biol*. 2004;49:R13–R48.
- Massoud TF, Gambhir SS. Molecular imaging in living subjects: seeing fundamental biological processes in a new light. *Genes Dev*. 2003;17:545–580.
- Gambhir SS, Barrio JR, Phelps ME, et al. Imaging adenoviral-directed reporter gene expression in living animals with positron emission tomography. *Proc Natl Acad Sci USA*. 1999;96:2333–2338.
- Wyss MT, Honer M, Schubiger PA, Ametamey SM. NanoPET imaging of [<sup>18</sup>F]fluoromisonidazole uptake in experimental mouse tumours. *Eur J Nucl Med Mol Imaging*. 2006;33:311–318.
- Ginovart N, Sun W, Wilson A, Houle S, Kapur S. Quantitative validation of an intracerebral beta-sensitive microprobe system to determine in vivo drug-induced receptor occupancy using [<sup>11</sup>C]raclopride in rats. *Synapse*. 2004;52:89–99.
- Zimmer L, Hassoun W, Pain F, et al. SIC, an intracerebral beta+ -range-sensitive probe for radiopharmacology investigations in small laboratory animals: binding studies with [<sup>11</sup>C]raclopride. *J Nucl Med*. 2002;43:227–233.
- Zimmer L, Pain F, Mauger G, et al. The potential of the beta-MICROPROBE, an intracerebral radiosensitive probe, to monitor the [<sup>18</sup>F]MPPF binding in the rat dorsal raphe nucleus. *Eur J Nucl Med Mol Imaging*. 2002;29:1237–1247.
- Zimmer L, Mauger G, Le Bars D, Bonmarchand G, Luxen A, Pujol J. Effect of endogenous serotonin on the binding of the 5-HT<sub>1A</sub> PET ligand [<sup>18</sup>F]-MPPF in the rat hippocampus: kinetic beta measurements combined with microdialysis. *J Neurochem*. 2002;80:278–286.
- Rbah L, Levie V, Zimmer L. Displacement of the PET ligand [<sup>18</sup>F]-MPPF by the electrically evoked serotonin release in the rat hippocampus. *Synapse*. 2003;49:239–245.
- Zimmer L, Riad M, Rbah L, et al. Toward brain imaging of serotonin 5-HT<sub>1A</sub> autoreceptor internalization. *Neuroimage*. 2004;22:1421–1426.
- Pain F, Besret L, Vaufrey F, et al. In vivo quantification of localized neuronal activation and inhibition in the rat brain using a dedicated high temporal resolution beta-sensitive MICROPROBE. *Proc Natl Acad Sci USA*. 2002;99:10807–10812.
- Millet P, Moulin Sallanon M, Petit J, et al. In vivo measurement of glucose utilization in rats using a beta-Microprobe: direct comparison with autoradiography. *J Cereb Blood Flow Metab*. 2004;24:1015–1024.
- Weber B, Spath N, Wyss M, et al. Quantitative cerebral blood flow measurements in the rat using a beta-probe and H<sub>2</sub><sup>15</sup>O. *J Cereb Blood Flow Metab*. 2003;23:1455–1460.
- Plenevaux A, Weissmann D, Aerts J, et al. Tissue distribution, autoradiography, and metabolism of (4-(2'-methoxyphenyl)-1-[2'-(N-2-pyridinyl)-p-[<sup>18</sup>F]fluorobenzamido]-ethyl]piperazine, p-[<sup>18</sup>F]-MPPF, a new serotonin 5-HT<sub>1A</sub> antagonist for positron emission tomography: an in vivo study in rats. *J Neurochem*. 2000;75:803–811.
- Aznavour N, Zimmer L. [<sup>18</sup>F]MPPF as a tool for the in vivo imaging of 5-HT<sub>1A</sub> receptor in animal and human brain. *Neuropharmacology*. 2007;52:695–707.
- Toth M. 5-HT<sub>1A</sub> receptor knockout mouse as a genetic model of anxiety. *Eur J Pharmacol*. 2003;463:177–184.
- Overstreet DH, Commisaris RC, De La Garza R, File SE, Knapp DJ, Seiden LS. Involvement of 5-HT<sub>1A</sub> receptors in animal tests of anxiety and depression: evidence from genetic models. *Stress*. 2003;6:101–110.
- Agostinelli S, Allison J, Amako K, et al. Geant4: a simulation toolkit. *Nucl Instrum Methods Phys Res A*. 2003;506:250–303.
- Jan S, Santin G, Strul D, et al. GATE: a simulation toolkit for PET and SPECT. *Phys Med Biol*. 2004;49:4543–4561.
- Desbree A, Pain F, Gurden H, et al. A new multimodality system for quantitative in vivo studies in small animals: combination of nuclear magnetic resonance and the radiosensitive beta-MicroProbe. *IEEE Trans Nucl Sci*. 2005;52:1281–1287.
- Le Bars D, Bonmarchand G, Alvarez J, Lemaire C, Mosdzianowski C. New automation of [<sup>18</sup>F]-MPPF using a coincidence synthesizer [abstract]. *J Labelled Comp Radiopharm*. 2001;44(suppl):S1045.
- Desbree A, Rbah L, Langlois J, et al. Simultaneous in vivo magnetic resonance imaging and radioactive measurements by the beta-Microprobe. *Eur J Nucl Med Mol Imaging*. 2007;34:1868–1872.
- Pain F, Lanièce P, Mastroioppo R, et al. SIC, an intracerebral radiosensitive probe for in vivo neuropharmacology investigations in small laboratory animals: theoretical considerations and physical characteristics. *IEEE Trans Nucl Sci*. 2000;47:25–32.
- Pain F, Lanièce P, Mastroioppo R, et al. SIC, an intracerebral radiosensitive probe for in vivo neuropharmacology investigations in small laboratory animals: first prototype design characterisation and in vivo evaluation. *IEEE Trans Nucl Sci*. 2002;49:822–826.
- Paxinos G, Franklin KBJ. *The Mouse Brain in Stereotaxic Coordinates*. San Diego, CA: Academic Press; 2001.
- Logan J, Fowler JS, Volkow ND, et al. Graphical analysis of reversible radioligand binding from time-activity measurements applied to [<sup>11</sup>C-methyl]-(-)-cocaine PET studies in human subjects. *J Cereb Blood Flow Metab*. 1990;10:740–747.
- Prima S, Ourselin S, Ayache N. Computation of the mid-sagittal plane in 3-D brain images. *IEEE Trans Med Imaging*. 2002;21:122–138.
- Dubois A, Dauguet J, Herard AS, et al. Automated three-dimensional analysis of histological and autoradiographic rat brain sections: application to an activation study. *J Cereb Blood Flow Metab*. 2007;27:1742–1755.
- Malakoff D. The rise of the mouse, biomedicine's model mammal. *Science*. 2000;288:248–253.
- Gingrich JA, Hen R. Dissecting the role of the serotonin system in neuropsychiatric disorders using knockout mice. *Psychopharmacology (Berl)*. 2001;155:1–10.
- Phelps ME. PET: the merging of biology and imaging into molecular imaging. *J Nucl Med*. 2000;41:661–681.
- Woody CL, Stoll SP, Schlyer DJ, et al. A study of scintillation beta microprobes. *IEEE Trans Nucl Sci*. 2002;49:2208–2212.
- Riad M, Zimmer L, Rbah L, Watkins KC, Hamon M, Descarries L. Acute treatment with the antidepressant fluoxetine internalizes 5-HT<sub>1A</sub> autoreceptors and reduces the in vivo binding of the PET radioligand [<sup>18</sup>F]MPPF in the nucleus raphe dorsalis of rat. *J Neurosci*. 2004;24:5420–5426.
- Aznavour N, Rbah L, Riad M, et al. PET imaging study of 5-HT<sub>1A</sub> receptors in cat brain after acute and chronic fluoxetine treatment. *Neuroimage*. 2006;33:834–842.
- Costes N, Merlet I, Zimmer L, et al. Modeling [<sup>18</sup>F]MPPF positron emission tomography kinetics for the determination of 5-hydroxytryptamine(1A) receptor concentration with multiinjection. *J Cereb Blood Flow Metab*. 2002;22:753–765.
- Lanfume L, Hamon M. 5-HT<sub>1</sub> receptors. *Curr Drug Targets CNS Neurol Disord*. 2004;3:1–10.
- Pain F, Lanièce P, Mastroioppo R, Gervais P, Hantraye P, Besret L. Arterial input function measurement without blood sampling using a beta-microprobe in rats. *J Nucl Med*. 2004;45:1577–1582.



The Journal of  
NUCLEAR MEDICINE

## The Potential of a Radiosensitive Intracerebral Probe to Monitor $^{18}\text{F}$ -MPPF Binding in Mouse Hippocampus In Vivo

Aurélie Desbrée, Mathieu Verdurand, Jeremy Godart, Albertine Dubois, Roland Mastroioppo, Frédéric Pain, Laurent Pinot, Thierry Delzescaux, Hirc Gurden, Luc Zimmer and Philippe Lanière

*J Nucl Med.* 2008;49:1155-1161.  
Published online: June 13, 2008.  
Doi: 10.2967/jnumed.107.050047

---

This article and updated information are available at:  
<http://jnm.snmjournals.org/content/49/7/1155>

---

Information about reproducing figures, tables, or other portions of this article can be found online at:  
<http://jnm.snmjournals.org/site/misc/permission.xhtml>

Information about subscriptions to JNM can be found at:  
<http://jnm.snmjournals.org/site/subscriptions/online.xhtml>

*The Journal of Nuclear Medicine* is published monthly.  
SNMMI | Society of Nuclear Medicine and Molecular Imaging  
1850 Samuel Morse Drive, Reston, VA 20190.  
(Print ISSN: 0161-5505, Online ISSN: 2159-662X)

© Copyright 2008 SNMMI; all rights reserved.